The Energy Spectrum of Ultra-High-Energy Cosmic Rays across Declinations from −90° to +44.8° Measured at the Pierre Auger Observatory

Fabio Convenga on behalf of the Pierre Auger Collaboration

PIERRE AUGER OBSERVATORY

INFN Laboratori Nazionali del Gran Sasso

GSSI GRAN SASSO SCIENCE INSTITUTE

TeV Particle Astrophysics TeVPA 2026

The UHECR Energy Spectrum Across Declinations

Phys. Rev. Lett. 135, 241002 (2025)

Ultra-high-energy cosmic rays exhibit a complex energy spectrum characterized by several changes in slope:

- the **ankle** around 5 EeV,
- the **instep** around 13 EeV,
- the strong flux **suppression** above approximately 48 EeV.

A 6.8σ dipole is observed above 8 EeV, with intermediate-scale hints at higher energies.

A few dominant nearby sources could imprint different spectral shapes across the sky.

Does the energy spectrum change with declination?

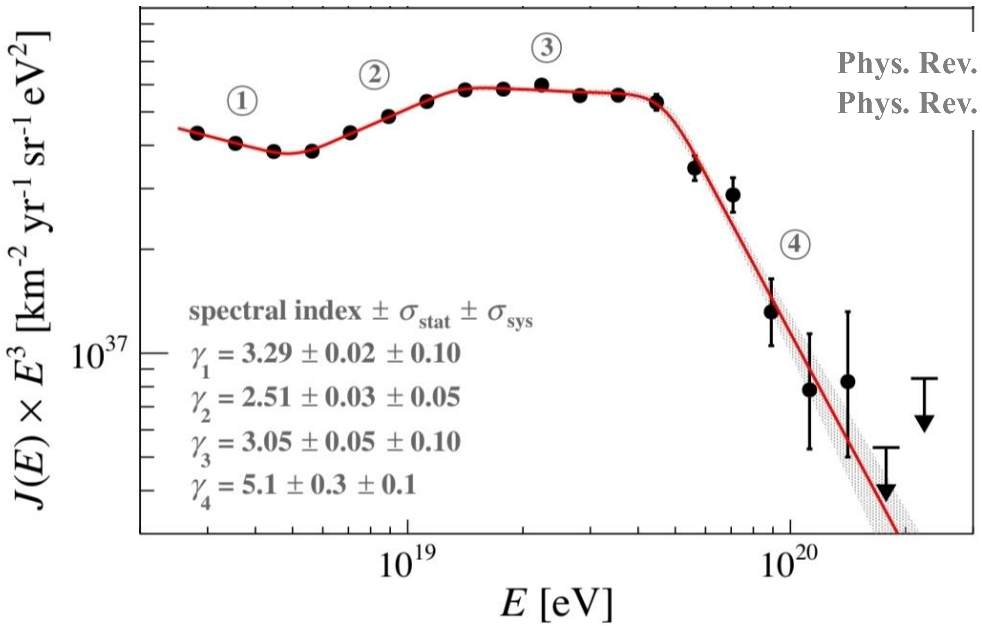

Phys. Rev. D 102, 062005 (2020)
Phys. Rev. Lett. 125, 121106 (2020)

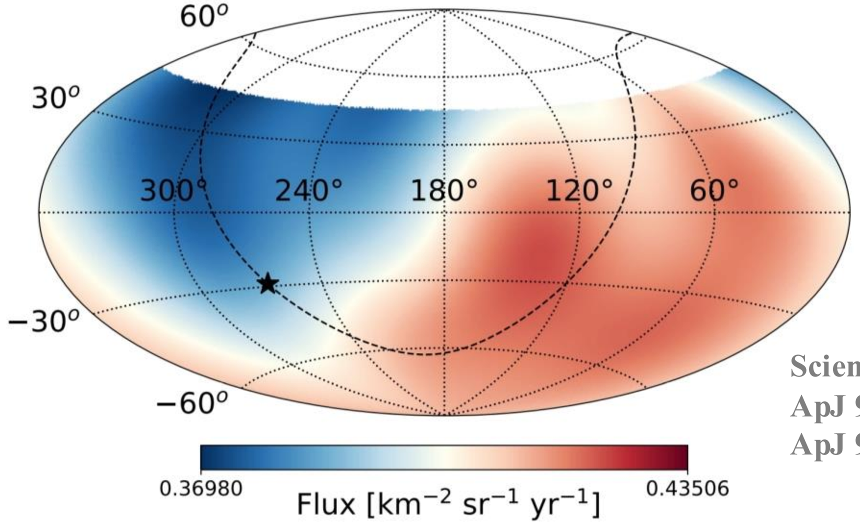

Science 357, 1266 (2017)
ApJ 976, 48
ApJ 935, 170 (2022)

Multi-hybrid detection

Fluorescence Detector (FD)
Duty Cycle ~ 13%

- Longitudinal profile
- Calorimetric Energy

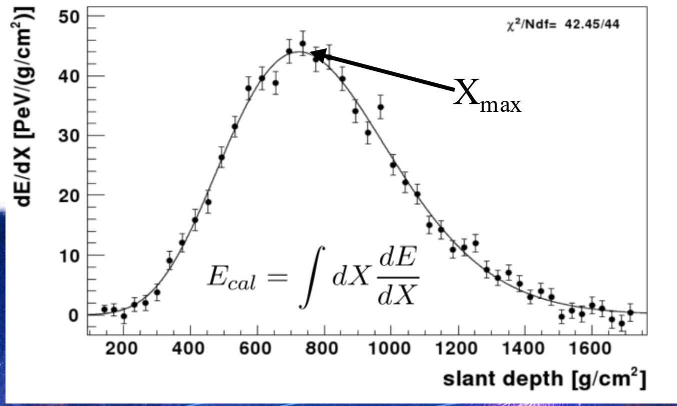

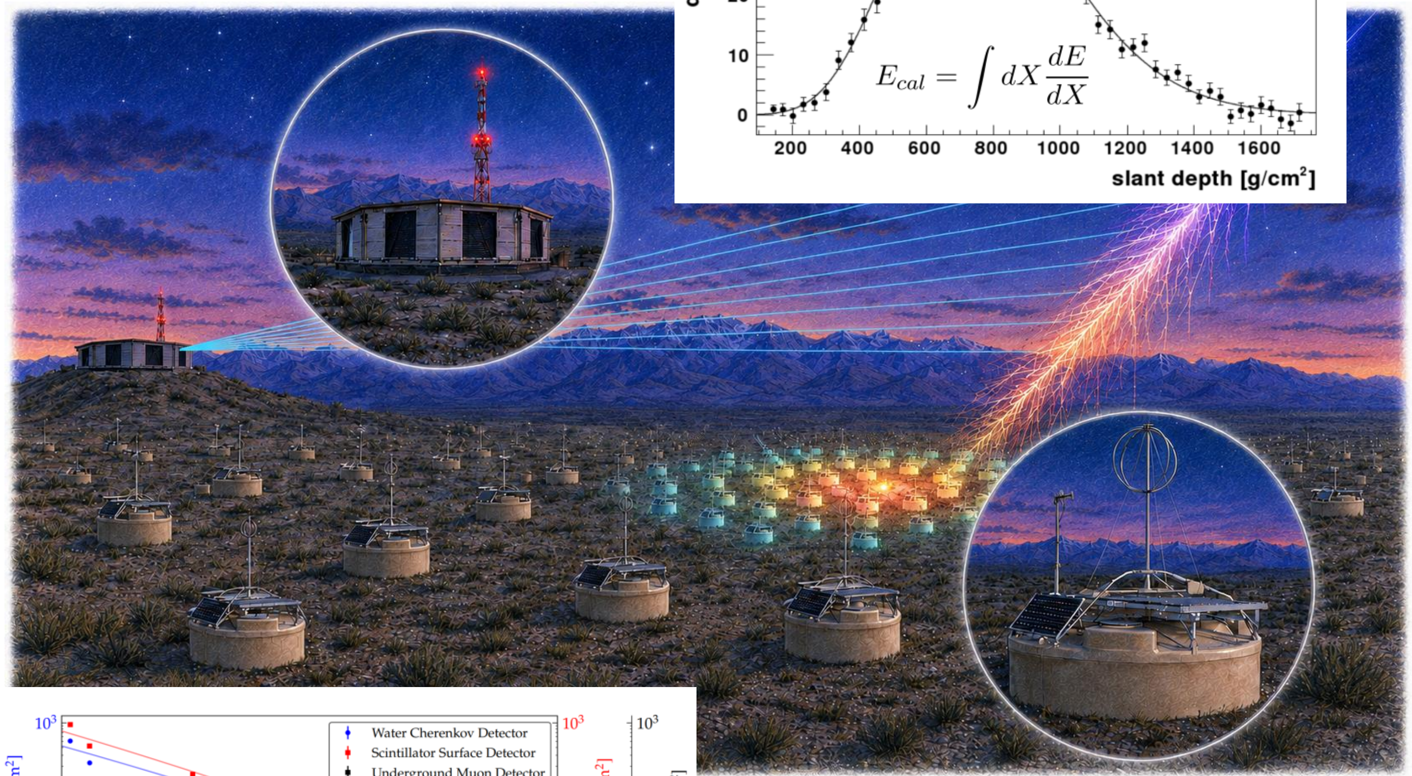

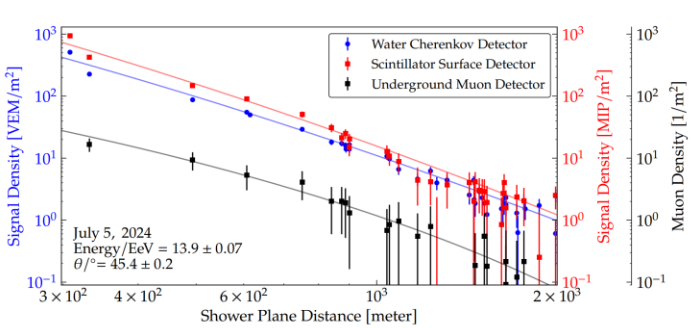

Surface Detector (SD)
Duty Cycle ~ 100%

- Lateral distributions of signals
- Several Energy estimators, for this work two are used: S(1000), N_{19}
- Since Phase II is now a multi-hybrid detector system

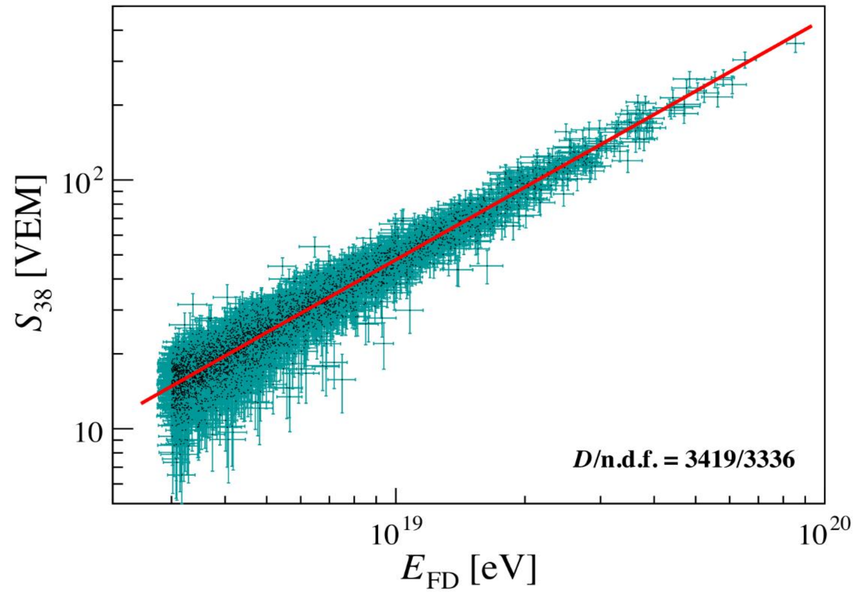

Hybrid energy calibration

Samples of high-quality hybrid events, simultaneously recorded by the SD and FD, are used to calibrate the two shower-size estimators:

$$S(1000) \xrightarrow{\text{CIC}} S_{38} \xrightarrow{\text{FD}} E_{\text{vert}} = A_S\, S_{38}^{B_S}$$

$$N_{19} \xrightarrow{\text{CIC}} N_{68} \xrightarrow{\text{FD}} E_{\text{incl}} = A_N\, N_{68}^{B_N}$$

The dependency on the zenith is removed

Two complementary SD-1500 datasets

Surface Detector data collected from January 2004 to December 2022

VERTICAL EVENTS 0°– 60°

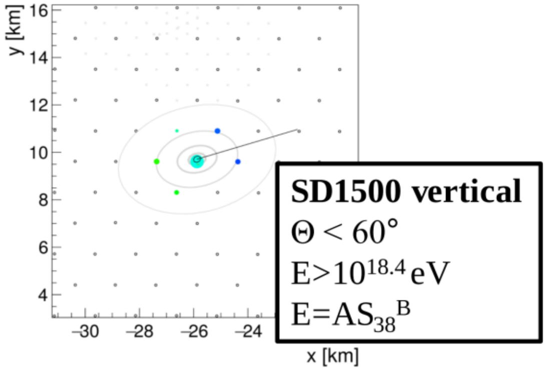

Nearly circular footprint

INCLINED EVENTS 60°– 80°

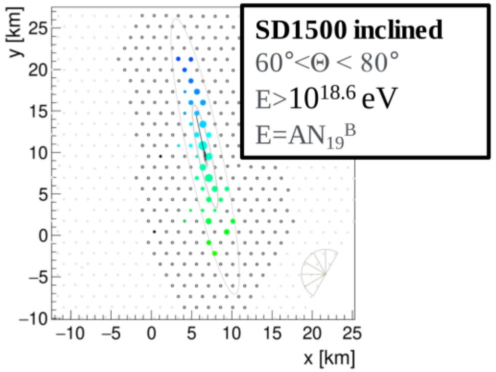

Muon-dominated, asymmetric footprint

COMMON FIELD OF VIEW: −84.8° ≤ δ ≤ +24.8°

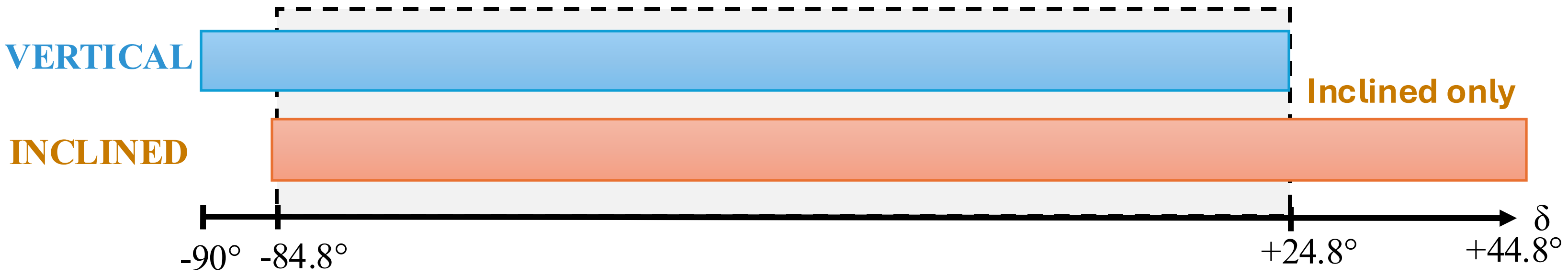

Inclined events provide fewer events, but extend the spectrum measurement northward to δ = +44.8°

Combination

Datasets are restricted to their common declination range:

$$-84.8° \leq \delta \leq +24.8°$$

An underlying spectrum is forward-folded through the two detector responses.

$$J(E;\mathbf{p}) = J_0 \left(\frac{E}{E_0}\right)^{-\gamma_0} \frac{\prod_{j=1}^{3}\left[1+\left(\frac{E}{E_{jk}}\right)^{\omega_{jk}^{-1}}\right]^{(\gamma_j-\gamma_k)\omega_{jk}}}{\prod_{j=1}^{3}\left[1+\left(\frac{E_0}{E_{jk}}\right)^{\omega_{jk}^{-1}}\right]^{(\gamma_j-\gamma_k)\omega_{jk}}}$$

Parameters	Role	Fit
J_0	Normalization	Free
$\gamma_1, \gamma_2, \gamma_3, \gamma_4$	Spectral indices	Free (4)
E_{12}, E_{23}, E_{34}	Turning energies	Free (3)
$\omega_{12}, \omega_{23}, \omega_{34}$	Transition widths	0.05
E_0	Pivot energy	$10^{0.5}$ EeV

$$\mathbf{p} = (J_0, \gamma_1, \gamma_2, \gamma_3, \gamma_4, E_{12}, E_{23}, E_{34})$$

p are adjusted to obtain the best match between the observed number of events in each energy bin and the expected ones simultaneously for both data streams.

The minimization procedure is based on the product of Poissonian likelihood functions:

$$\mathcal{L}(\mathbf{p},\mathbf{x}) = \underbrace{\mathcal{L}_{[0°,60°]}(\mathbf{p},\mathbf{x})}_{\text{vertical events}}\ \underbrace{\mathcal{L}_{[60°,80°]}(\mathbf{p},\mathbf{x})}_{\text{inclined events}}\ \underbrace{\mathcal{L}_x(\mathbf{x})}_{\text{calibration penalty}}$$

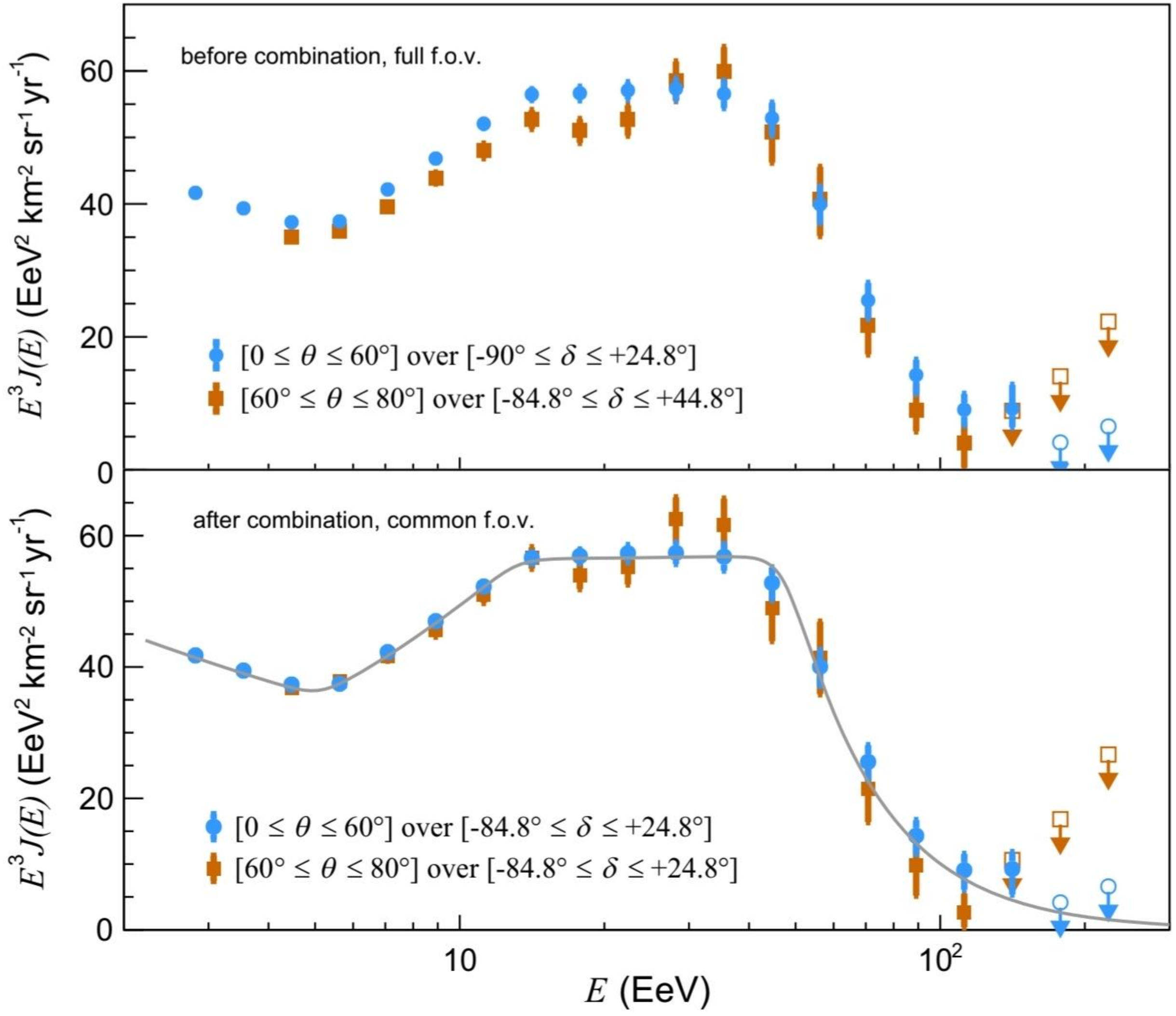

A constrained correction aligns the N_{68} energy scale

In the common field of view, the residual difference is treated as an independent calibration uncertainty, not as a free rescaling.

1 — Common systematics cannot explain a relative offset

Energy-scale, exposure and unfolding uncertainties move both spectra coherently.

2 — Only the independently calibrated inclined scale is adjusted

N_{68} uses lower statistics, the vertical scale remains the reference.

3 — Spectrum and calibration corrections are fitted simultaneously

A covariance-based penalty keeps every trial correction within the hybrid-calibration uncertainty.

Constrained correction of the N_{68} calibration

$$E = A\,N_{68}^{B} \quad \longrightarrow \quad E_{\mathrm{corr}} = \begin{cases} (A+\delta A)\,N_{68}^{B+\delta B}, & E \le 10\,\mathrm{EeV} \\ (A+\delta A)\,N_{68}^{B+\delta B+\delta C}, & E > 10\,\mathrm{EeV} \end{cases}$$

- δA normalization
- δB global slope
- δC nonlinearity above 10 EeV

Joint forward-folding fit

For each trial correction, the inclined energy bins and expected event counts are recomputed.

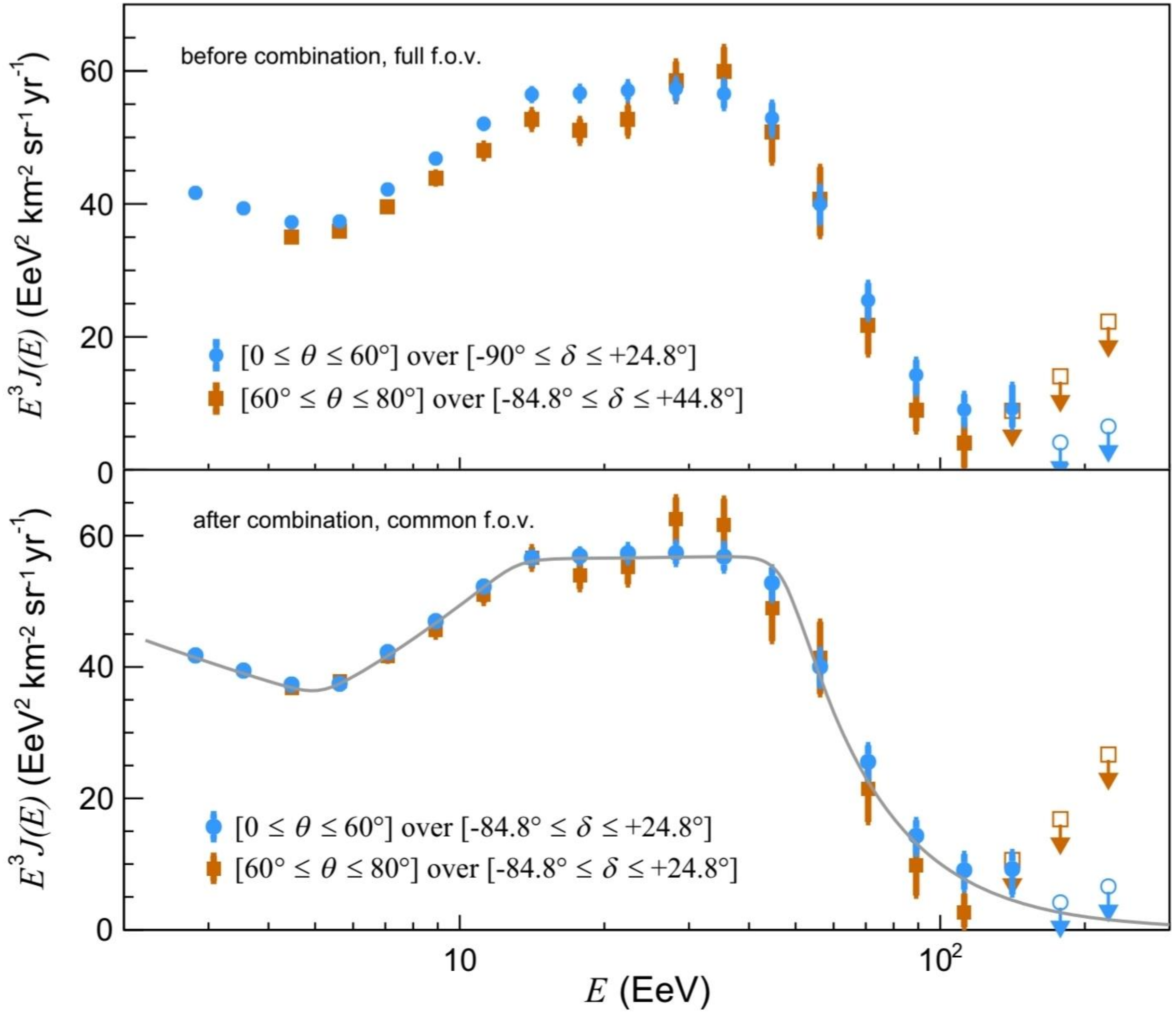

One underlying spectrum, two detector responses

The best-fit model provides the unfolding corrections used to combine the two event samples into a single spectrum.

2 **Correct bin migration**

Their ratio defines the unfolding correction for each energy bin.

3 **Build the combined flux**

Corrected vertical and inclined counts are divided by exposure and bin width.

Unfolding factor

$$c_i = \frac{\mu_i}{\nu_i}$$

Combined spectral point

$$J_i = \frac{c_i n_i^{[0^\circ,60^\circ]} + c_i n_i^{[60^\circ,80^\circ]}}{\mathcal{E}_i \, \Delta E_i}$$

Exposure:

Between 2.5 and 4 EeV, only the vertical dataset contributes.

Above 4 EeV, vertical and inclined events are combined.

This change reflects the different energy thresholds of the two datasets.

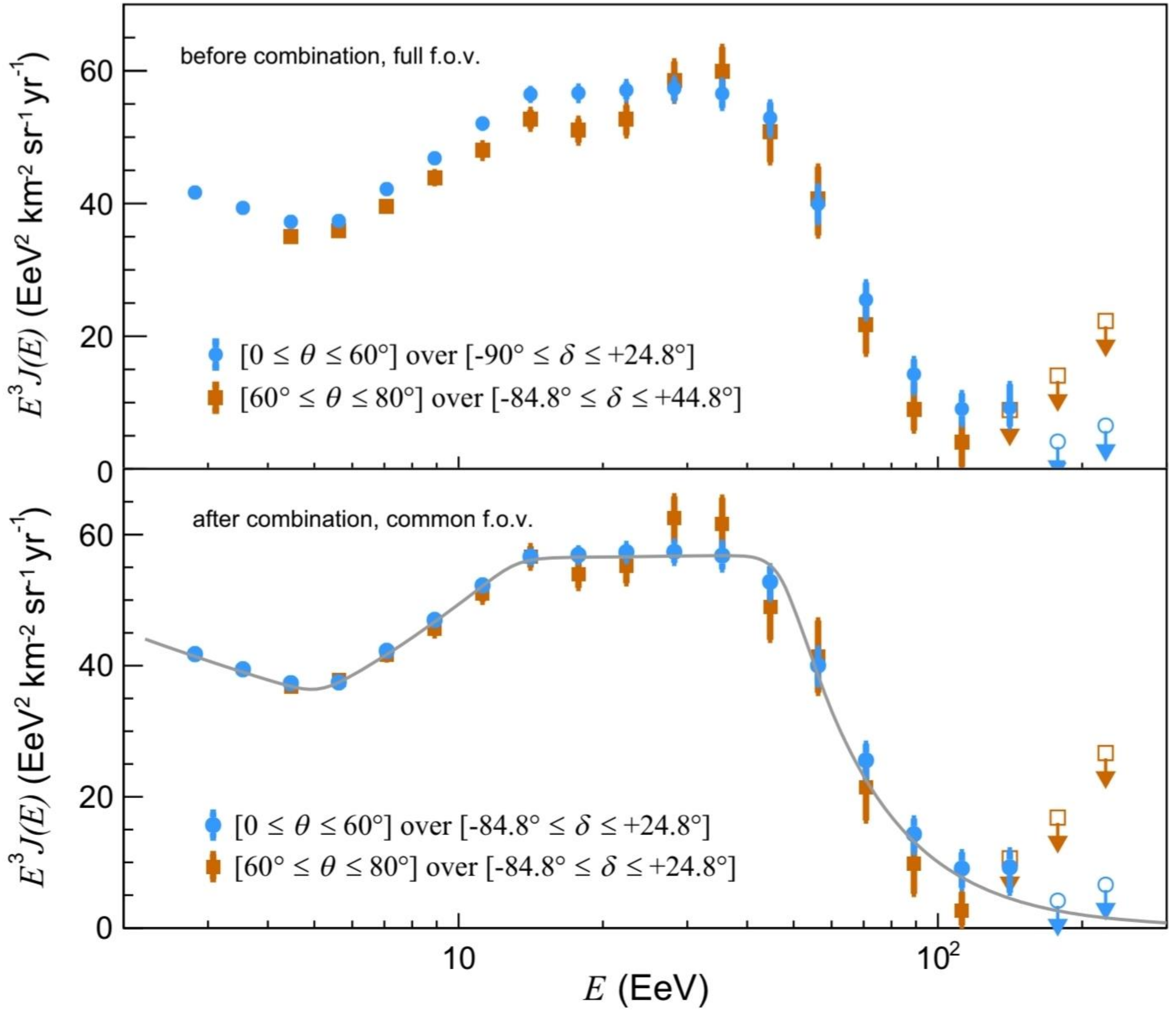

Five declination bands probe the full field of view

Declination bands

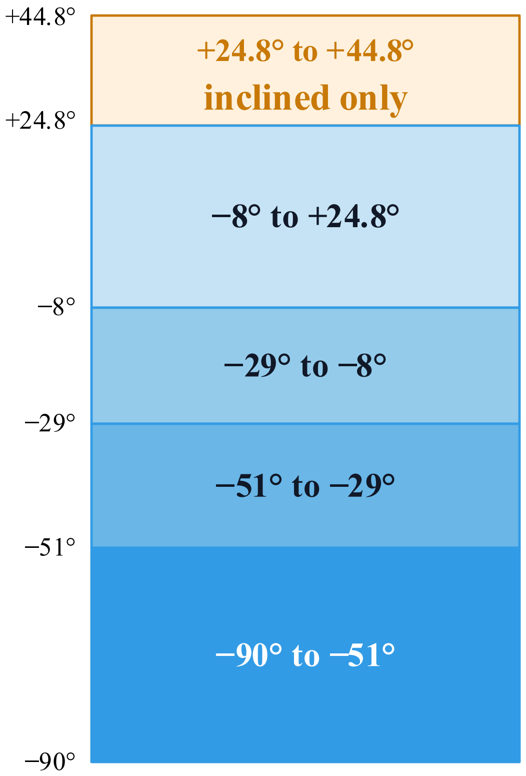

Comparable exposure

The four bands between −90° and +24.8° have exposures equal within 1%, averaging about 25,000 km² sr yr.

Northern extension

The +24.8° to +44.8° band contains inclined events only: 5,632 events above 4 EeV, with an exposure of (4,100 ± 120) km² sr yr.

Expected spectrum in one band

$J_{\Delta\delta}(E;\,p)$ is the reference spectrum modified by the measured dipole and averaged over the directional exposure of the selected band.

$$J_{\Delta\delta}(E;\mathbf{p}) = J(E;\mathbf{p})\left(1+\frac{\mathcal{E}_0}{\mathcal{E}_{\Delta\delta}}\,\frac{\int_{\Delta\delta} d\delta\,\cos\delta\,\omega(\delta) + d_z(E)\int_{\Delta\delta} d\delta\,\cos\delta\,\sin\delta\,\omega(\delta)}{\int d\delta\,\cos\delta\,\omega(\delta) + d_z(E)\int d\delta\,\cos\delta\,\sin\delta\,\omega(\delta)}\right)$$

ω(δ): directional exposure
$d_z(E)$: measured dipole component

Dotted curves: isotropic reference. Solid curves: expectation including the measured dipole

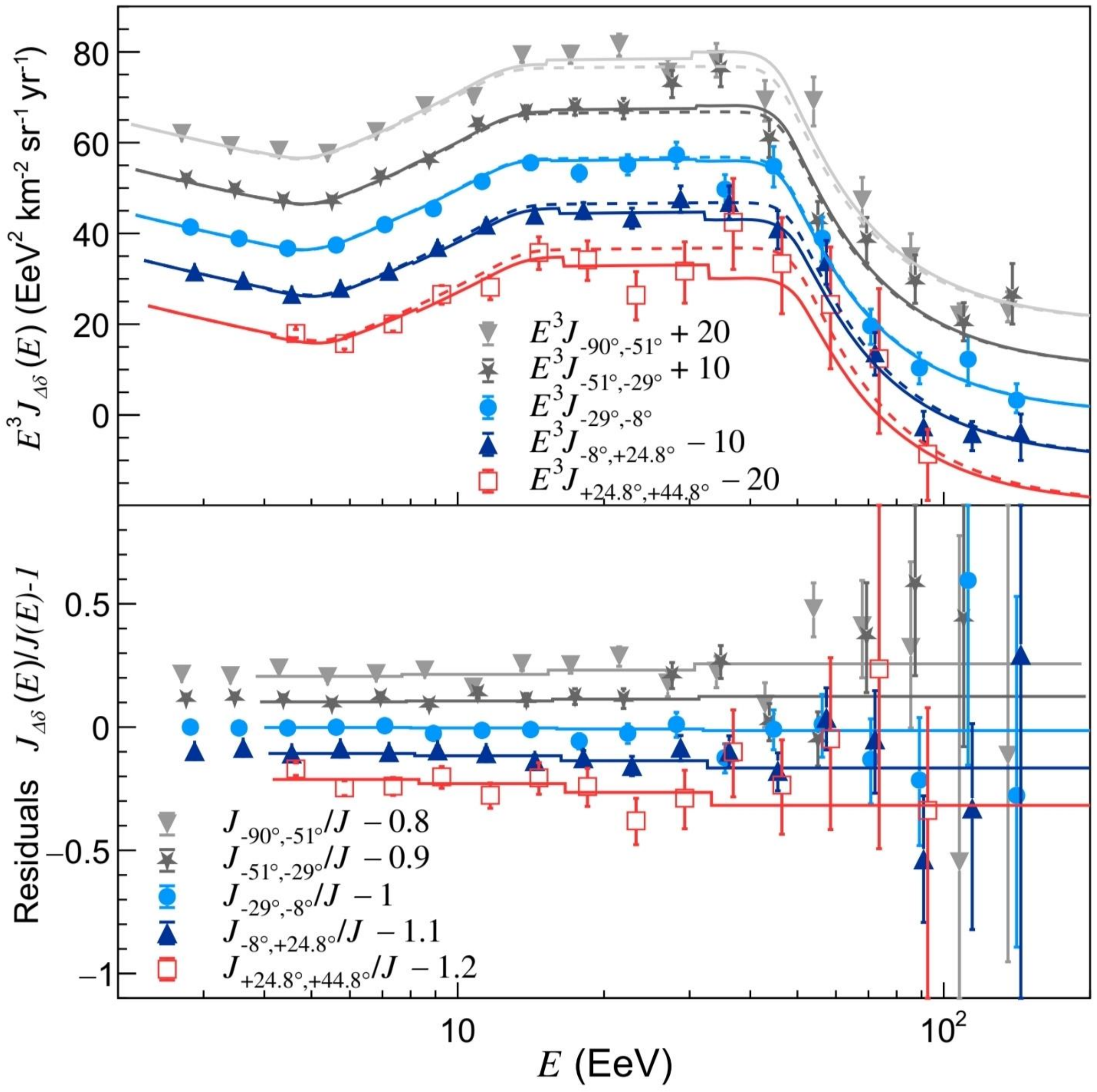

No significant spectral departure across declination bands

Each band yields its own spectrum $J_{\Delta\delta}(E;\, p_{\Delta\delta})$, which is then compared with the common reference.

One forward-folding fit per band

$$Q^2 = \left(\boldsymbol{p}_{\Delta\delta} - \boldsymbol{p}_{\mathrm{ref}}\right)^T \left(\Sigma_{\Delta\delta} + \Sigma_{\mathrm{ref}}\right)^{-1} \left(\boldsymbol{p}_{\Delta\delta} - \boldsymbol{p}_{\mathrm{ref}}\right)$$

It quantifies the difference between the spectral parameters fitted in each declination band and those of the reference spectrum, accounting for their uncertainties and correlations.

The corresponding probability is evaluated using simulated datasets.

No band shows a statistically significant departure.

The [−51°, −29°] band shows the mildest tension (P = 13%) in the high-energy parameters, but remains compatible.

$[\delta_{\min}, \delta_{\max}]$	J_0	γ_1	γ_2	γ_3	γ_4	E_{12}	E_{23}	E_{34}	$P(\geq Q^2)$ (%)
[−84.8°, +24.8°]	1.271 ± 0.004	3.26 ± 0.01	2.51 ± 0.03	2.99 ± 0.03	5.3 ± 0.2	5.1 ± 0.1	13 ± 1	48 ± 2	…
[−90°, −51°]	1.278 ± 0.007	3.24 ± 0.02	2.54 ± 0.06	3.18 ± 0.06	7.2 ± 1.0	5.1 ± 0.2	17 ± 2	62 ± 4	23
[−51°, −29°]	1.281 ± 0.007	3.26 ± 0.02	2.46 ± 0.06	2.87 ± 0.06	4.6 ± 0.4	5.2 ± 0.2	12 ± 2	39 ± 4	13
[−29°, −8°]	1.257 ± 0.007	3.28 ± 0.02	2.54 ± 0.06	3.02 ± 0.06	5.6 ± 0.4	4.9 ± 0.2	13 ± 2	49 ± 4	71
[−8°, +24.8°]	1.266 ± 0.007	3.26 ± 0.02	2.50 ± 0.06	2.97 ± 0.06	6.1 ± 0.4	5.1 ± 0.2	12 ± 2	51 ± 4	34
[+24.8°, +44.8°]	1.26 ± 0.03	3.26 (fixed)	2.6 ± 0.2	3.0 ± 0.2	11 ± 10	5.1 (fixed)	13 ± 4	69 ± 20	53

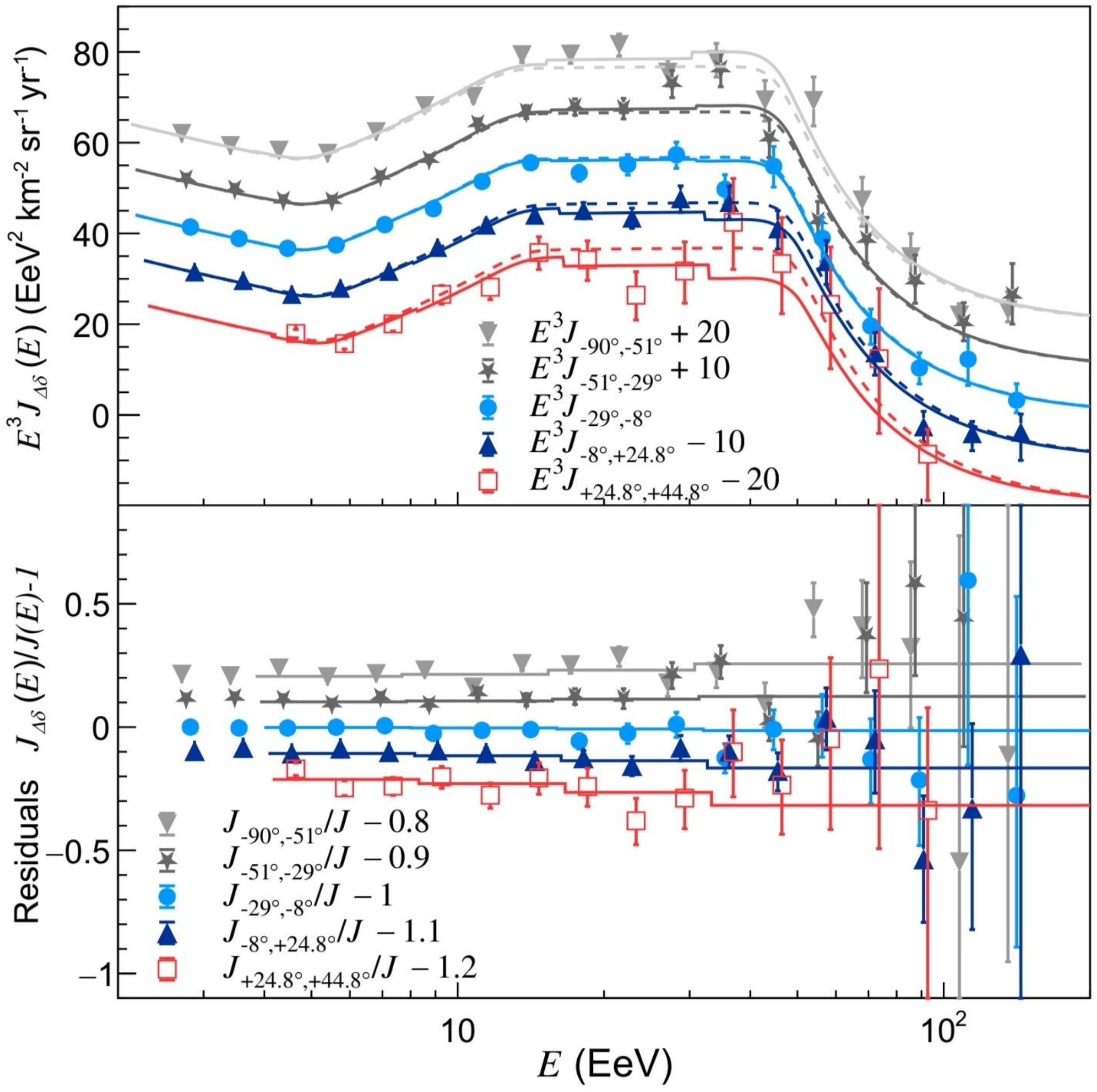

No significant spectral departure across declination bands

Each band yields its own spectrum $J_{\Delta\delta}(E;\, p_{\Delta\delta})$, which is then compared with the common reference.

One forward-folding fit per band

$$Q^2 = \left(\boldsymbol{p}_{\Delta\delta} - \boldsymbol{p}_{\mathrm{ref}}\right)^T \left(\Sigma_{\Delta\delta} + \Sigma_{\mathrm{ref}}\right)^{-1} \left(\boldsymbol{p}_{\Delta\delta} - \boldsymbol{p}_{\mathrm{ref}}\right)$$

It quantifies the difference between the spectral parameters fitted in each declination band and those of the reference spectrum, accounting for their uncertainties and correlations.

The corresponding probability is evaluated using simulated datasets.

No band shows a statistically significant departure.

The [−51°, −29°] band shows the mildest tension (P = 13%) in the high-energy parameters, but remains compatible.

$[\delta_{\min}, \delta_{\max}]$	J_0	γ_1	γ_2	γ_3	γ_4	E_{12}	E_{23}	E_{34}	$P(\geq Q^2)$ (%)
[−84.8°, +24.8°]	1.271 ± 0.004	3.26 ± 0.01	2.51 ± 0.03	2.99 ± 0.03	5.3 ± 0.2	5.1 ± 0.1	13 ± 1	48 ± 2	⋯
[−90°, −51°]	1.278 ± 0.007	3.24 ± 0.02	2.54 ± 0.06	3.18 ± 0.06	7.2 ± 1.0	5.1 ± 0.2	17 ± 2	62 ± 4	23
[−51°, −29°]	1.281 ± 0.007	3.26 ± 0.02	2.46 ± 0.06	2.87 ± 0.06	4.6 ± 0.4	5.2 ± 0.2	12 ± 2	39 ± 4	13
[−29°, −8°]	1.257 ± 0.007	3.28 ± 0.02	2.54 ± 0.06	3.02 ± 0.06	5.6 ± 0.4	4.9 ± 0.2	13 ± 2	49 ± 4	71
[−8°, +24.8°]	1.266 ± 0.007	3.26 ± 0.02	2.50 ± 0.06	2.97 ± 0.06	6.1 ± 0.4	5.1 ± 0.2	12 ± 2	51 ± 4	34
[+24.8°, +44.8°]	1.26 ± 0.03	3.26 (fixed)	2.6 ± 0.2	3.0 ± 0.2	11 ± 10	5.1 (fixed)	13 ± 4	69 ± 20	53

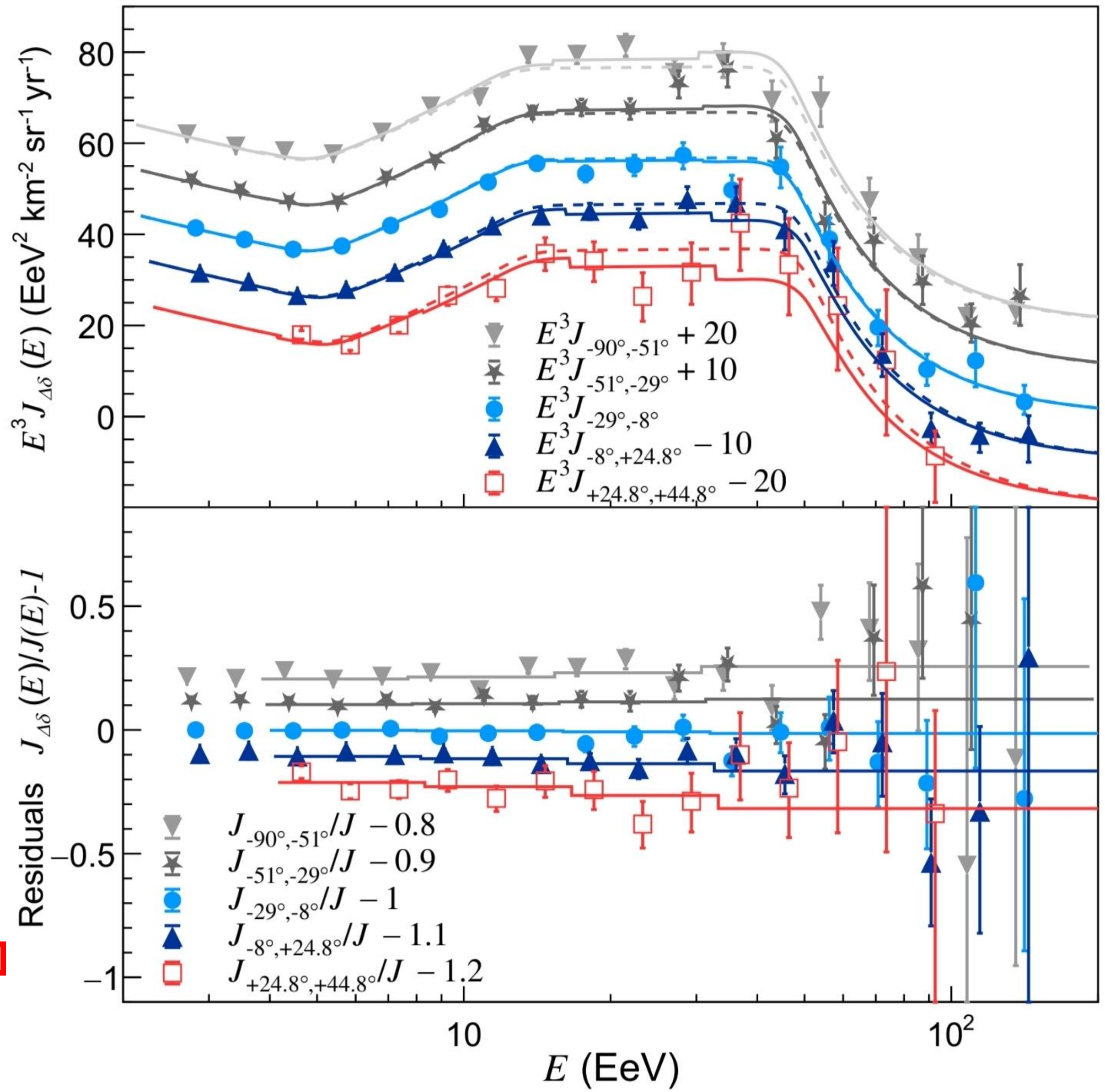

No significant spectral departure across declination bands

The [−51°, −29°] band has the lowest p-value (13%)

Centaurus A (α = 201°, δ = −43°) lies within in the band, in a region where a significant intermediate-scale overdensity has been reported. A. Abdul Halim et al., ApJ 984, 123 (2025)

Dedicated fit in a ≃24° window

Inside the Centaurus A window

$\gamma_3 = 2.8 \pm 0.3$
$E_{34} = (67 \pm 11)$ EeV
$\gamma_4 = 9 \pm 4$

Rest of the declination band

$\gamma_3 = 2.88 \pm 0.07$
$E_{34} = (37 \pm 4)$ EeV
$\gamma_4 = 4.5 \pm 0.5$

The window favours a later suppression and a steeper final index, but the uncertainties are too large to establish a significant difference.

Other source-centred checks

NGC 253	$E_{34} = (41 \pm 11)$ EeV, $\gamma_4 = 5 \pm 1$
NGC 1068	$E_{34} = (58 \pm 18)$ EeV, $\gamma_4 = 5 \pm 1$

The mild band-level tension cannot be attributed to Centaurus A, or to the other tested overdensities, with statistical significance.

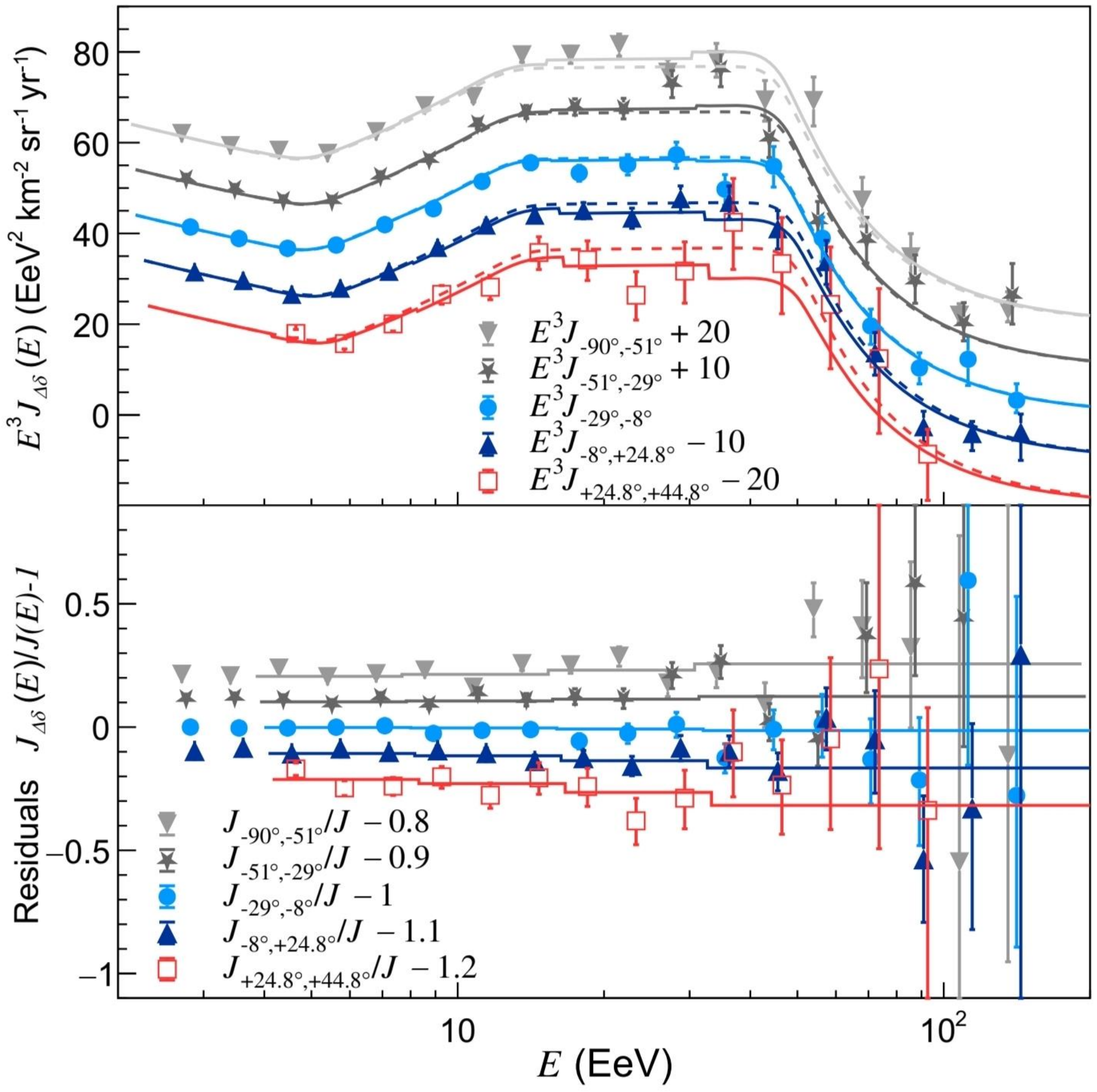

A single spectrum describes the full declination range

Having found no significant spectral dependence on declination, the full vertical and inclined datasets are combined on the aligned energy scale to construct a single spectrum

Three spectral features

Ankle

E_{12} = (5.1 ± 0.1 ± 1.1) EeV

Hardening from γ_1 to γ_2

Instep

E_{23} = (13 ± 1 ± 2) EeV

A subtle additional steepening

Flux suppression

E_{34} = (48 ± 2 ± 5) EeV

Rapid fall-off at the highest energies

The instep significance increases from 3.9σ to 5.5σ.

First uncertainty: statistical
Second: systematic

Spectrum across −90° ≤ δ ≤ +44.8°

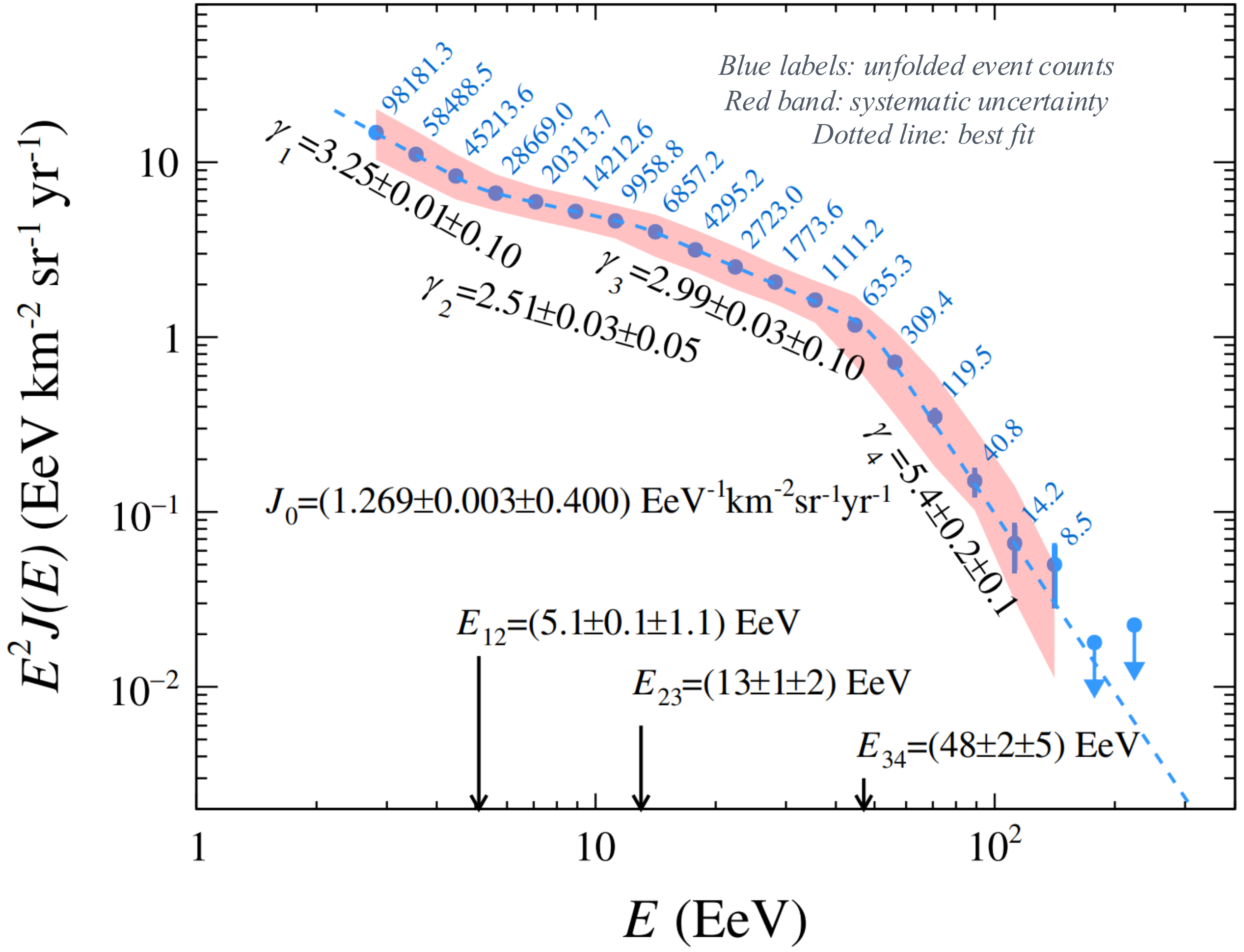

Interpretation

A joint fit connects the observed features to the superposition of propagated mass groups.

Astrophysical implications

Mixed

Mixed composition is favoured

Pure-proton models fail to fit the data

Rigidity

$\mathbf{E_{max} \propto Z}$

Maximum energy scales with particle charge

Heavy nuclei

Dominate at the highest energies

Short horizons favour nearby sources

Observed features arise from the superposition of propagated mass groups.

Joint fit of spectrum and composition

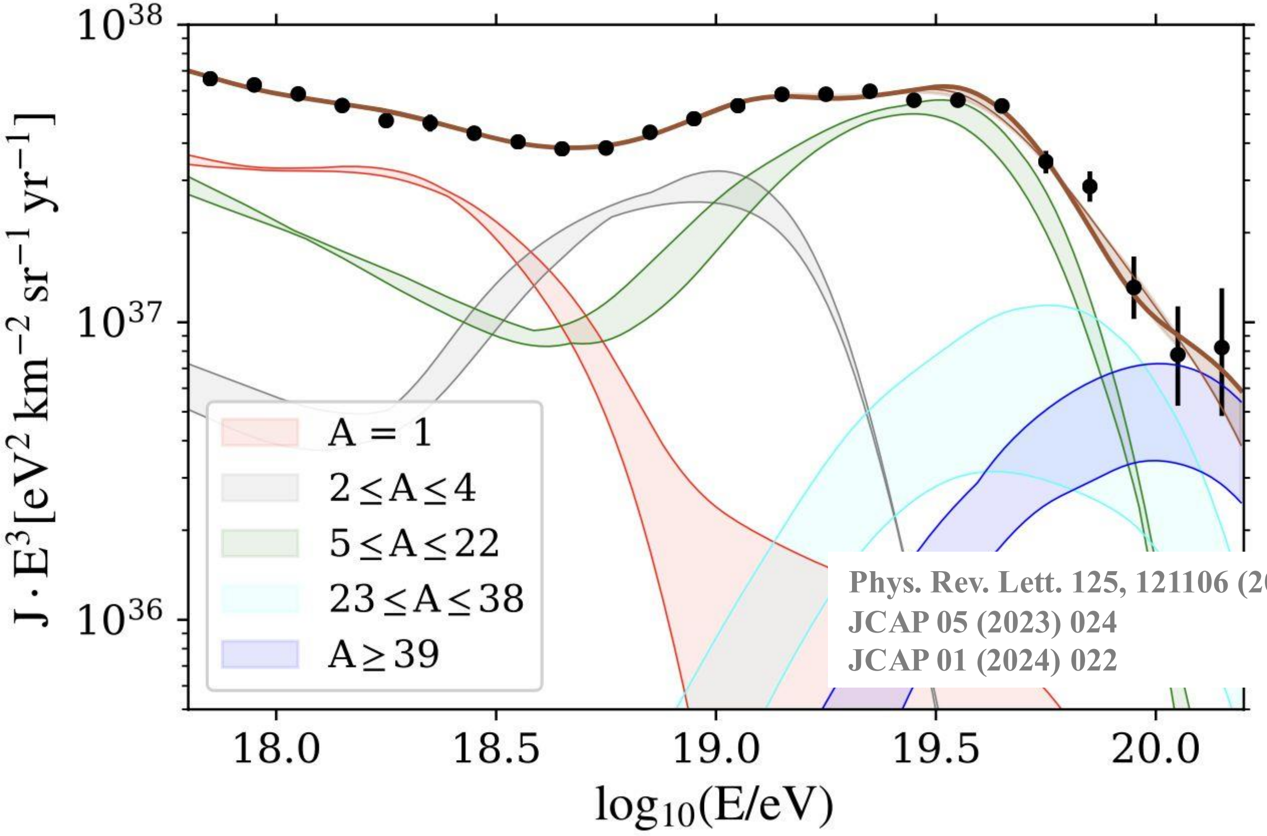

Phys. Rev. Lett. 125, 121106 (2020)
JCAP 05 (2023) 024
JCAP 01 (2024) 022

Summary

Two calibrated SD-1500 datasets provide one consistent measurement across the full accessible sky.

Four take-home results

1 DATASET & SKY COVERAGE

>310,000 events · −90° ≤ δ ≤ +44.8°

Vertical and inclined SD-1500 datasets

2 COMBINATION

Joint forward-folding fit

Common energy scale; detector migration unfolded

3 DIRECTIONAL TESTS

Five bands + source-centred checks

No statistically significant spectral departure

SPECTRAL FEATURES

5.1 EeV ankle · 13 EeV instep · 48 EeV suppression

The instep is established at 5.5σ.

An origin of the instep from a small number of dominant sources is disfavored.

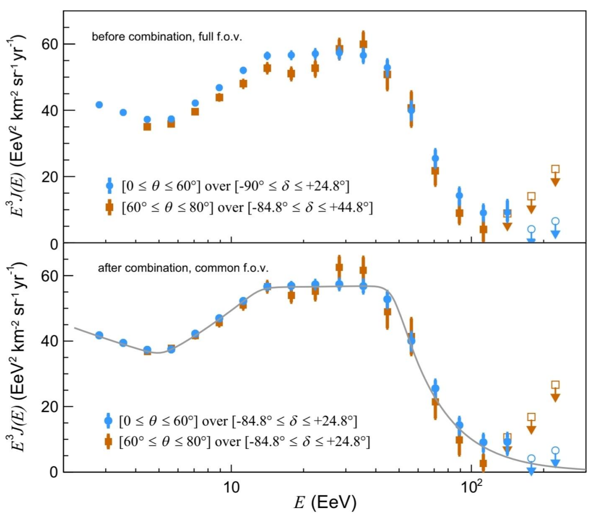

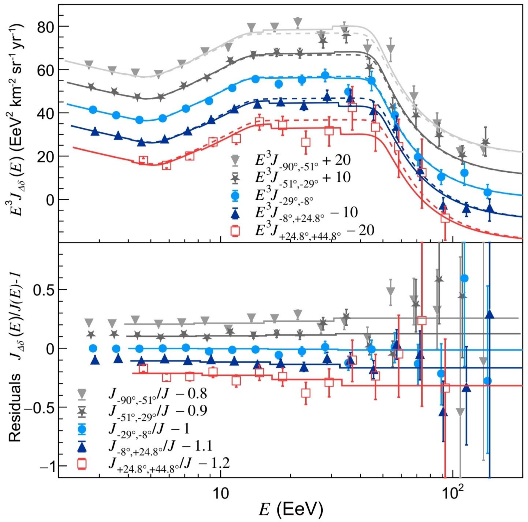

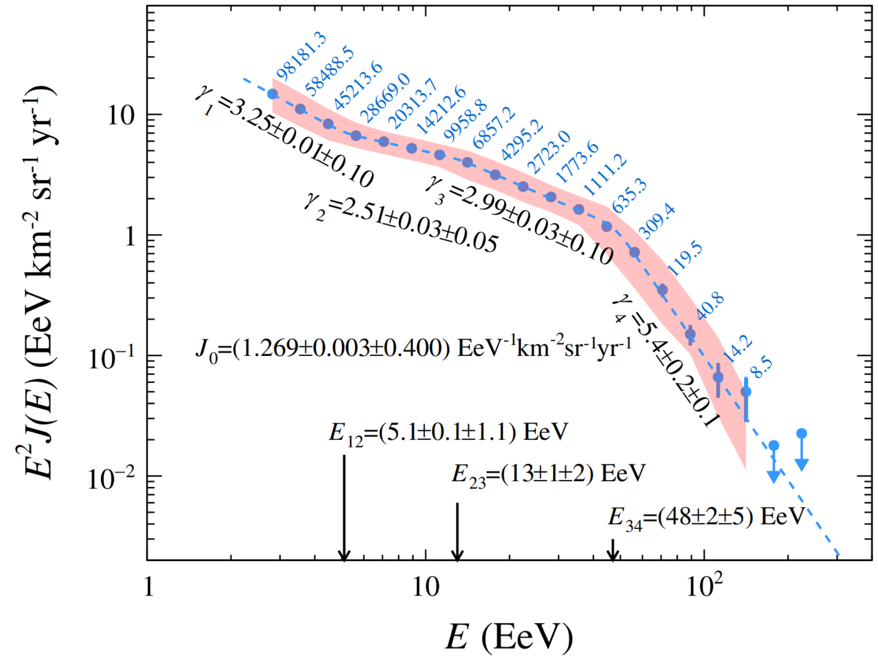

ありがとう ございます

Backup Slides

Pierre Auger Observatory and Telescope Array Spectrum

Achievements

A common fluorescence yield and invisible-energy correction reduce the discrepancy below .

The spectra agree within approximately 4% across most of the energy range.

Open question

A residual HE difference of about 20%.

Its origin is under investigation by the Auger–TA Working Group.

Possible systematic contribution

Potential mass-dependent calibration effects are being studied.

A realistic energy-dependent composition could reduces calibration biases.